Figure S1. (a) Fitting results of measured data points using different fitting methods. (**b**) Vertical section image of a single asperity.

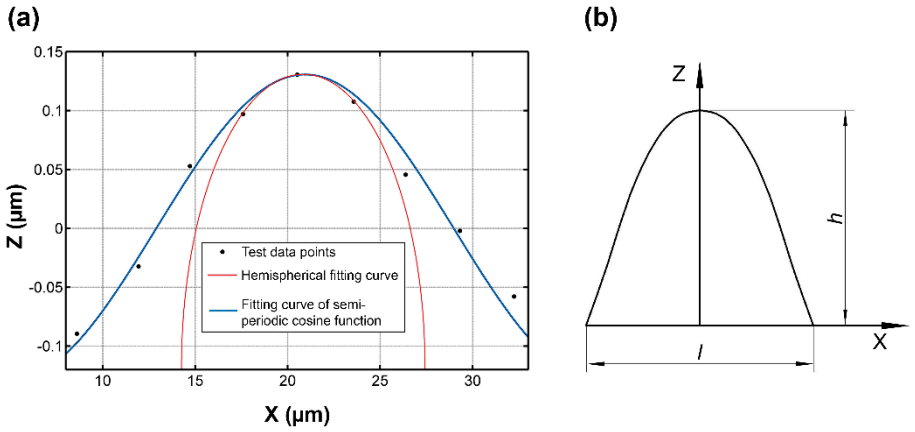


Figure S1. (a) Fitting results of measured data points using different fitting methods. (**b**) Vertical section image of a single asperity [1].

The fitting result shows that when the hemispherical geometry is used to fit the data points of the asperity, the fitting curve can fit well around the peak point. However, a complete fit from the geometry peak point to the valley point could not be achieved. That is to say, the current fitting result of an actual asperity geometry had local characteristics that were not reflected by the overall characteristics.

In this investigation, a cosine curve is used to fit the collection of points of the whole profile of a single asperity on the grinding surface. Such a fitting result is shown in Figure 2(a). It can be seen that a complete fitting from a valley point to a peak point to a valley point can be achieved using a cosine curve. By randomly selecting a single-asperity geometry for data fitting, it was found that the root mean square (RMS) error between the cosine function fitting curve and the data points can be controlled to less than 3%, whereas the error of the semicircular curve is above 12%. Therefore, in the present work, a semiperiodic cosine-curve revolving body was used in place of the already existing hemispherical and semiellipsoidal asperity geometry hypotheses. The vertical section of the semiperiodic cosine-curve revolving body can be found in Figure 2(b).

Figure S2. Measured grinding surfaces under different grinding wheels: (**a**) The specimen under 120#; (**b**) The actual surface of the measured area; (**c**) The surface topography of the measured area.

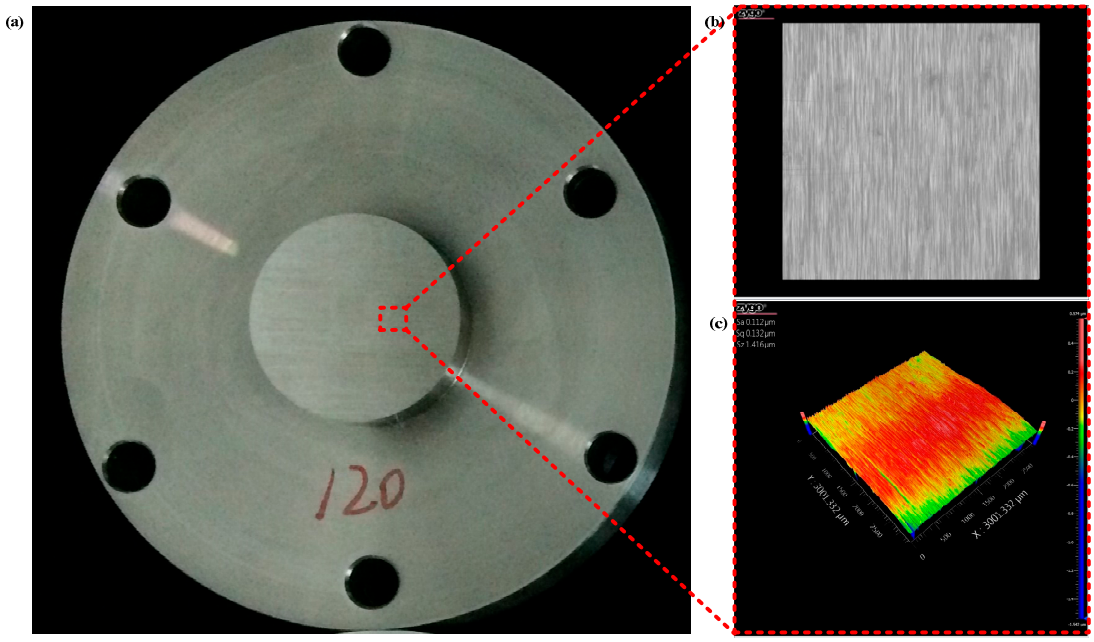


Figure S2. Measured grinding surfaces under different grinding wheels: (**a**) The specimen under 120#; (**b**) The actual surface of the measured area; (**c**) The surface topography of the measured area.

Figure S3. Measured grinding surfaces under different grinding wheels: (**a**) Surface 1; (**b**) Surface 2; (**c**) Surface 3; (**d**) Surface 4.

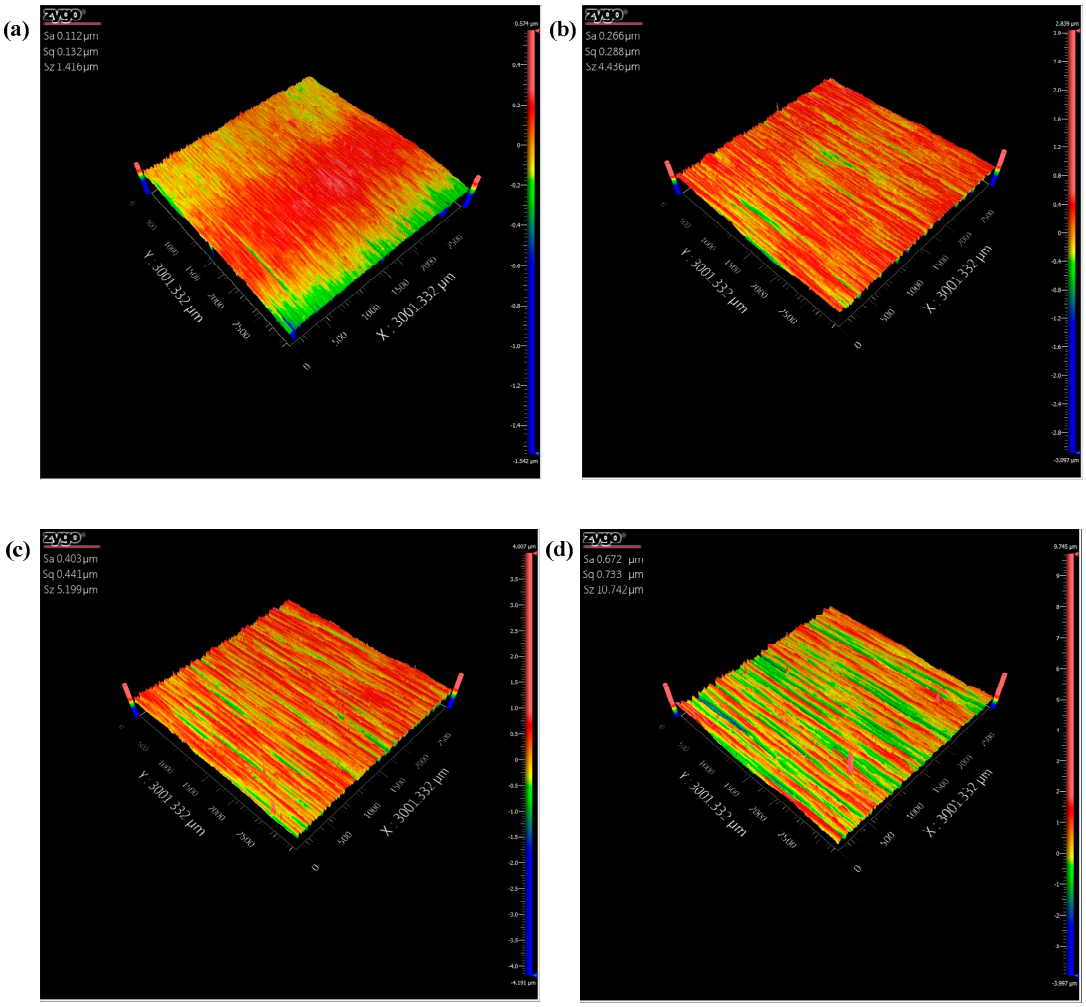


Figure S3. Measured grinding surfaces under different grinding wheels: (**a**) Surface 1; (**b**) Surface 2; (**c**) Surface 3; (**d**) Surface 4.

Table S1. The values and the relative errors of contact stiffness - Grinding joint surface 1

Contact pressure (MPa)	Contact stiffness (MPa/μm)			Relative errors (%)	
	Experimental results	Presented model results	KE model results	Presented model	KE model
0.00	0.00	0.00	0.00	0.00	0.00
10.00	19.51	19.12	20.31	2.02	4.06
20.00	40.45	38.52	38.08	4.77	5.87
30.00	58.69	56.20	54.52	4.25	7.11
40.00	72.61	72.16	69.24	0.62	4.65
50.00	92.34	88.40	82.22	4.27	10.96
60.00	106.62	103.91	93.48	2.54	12.32
70.00	122.20	118.71	103.01	2.86	15.71

Table S2. The values and the relative errors of contact stiffness - Grinding joint surface 2

Contact pressure (MPa)	Contact stiffness (MPa/μm)			Relative errors (%)	
	Experimental results	Presented model results	KE model results	Presented model	KE model
0.00	0.00	0.00	0.00	0.00	0.00
10.00	17.37	16.97	17.10	2.30	1.55
20.00	34.41	33.31	32.72	3.20	4.90
30.00	51.60	49.00	46.85	5.04	9.20
40.00	66.96	64.06	59.50	4.33	11.13
50.00	81.47	78.47	70.66	3.68	13.27
60.00	94.14	92.24	80.34	2.02	14.67
70.00	107.98	105.38	88.52	2.41	18.02

Table S3. The values and the relative errors of contact stiffness - Grinding joint surface 3

Contact pressure (MPa)	Contact stiffness (MPa/μm)			Relative errors (%)	
	Experimental results	Presented model results	KE model results	Presented model	KE model
0.00	0.00	0.00	0.00	0.00	0.00
10.00	13.28	13.38	13.17	0.75	0.81
20.00	26.81	26.20	24.97	2.26	6.85
30.00	38.56	38.46	35.38	0.26	8.23
40.00	50.56	50.16	44.42	0.79	12.15
50.00	63.79	61.30	52.07	3.91	18.38
60.00	72.28	71.88	58.34	0.56	19.29
70.00	80.01	81.88	63.23	2.33	20.97

Table S4. The values and the relative errors of contact stiffness - Grinding joint surface 4

Contact pressure (MPa)	Contact stiffness (MPa/μm)			Relative errors (%)	
	Experimental results	Presented model results	KE model results	Presented model	KE model

0.00	0.00	0.00	0.00	0.00	0.00
10.00	11.59	11.18	11.28	3.57	2.75
20.00	22.56	21.54	22.54	4.56	0.11
30.00	33.01	31.56	31.79	4.38	3.70
40.00	41.90	41.27	39.53	1.51	5.65
50.00	53.55	50.64	45.76	5.44	14.56
60.00	61.32	59.69	50.47	2.66	17.70
70.00	69.70	68.41	53.67	1.84	22.99

1. An, Q.; Suo, S.F.; Lin, F.Y.; Shi, J.W. A Novel Micro-Contact Stiffness Model for the Grinding Surfaces of Steel Materials Based on Cosine Curve-Shaped Asperities. *Materials* **2019**, *12*, 3561, doi:10.3390/ma12213561.